Published in final edited form as:

Cancer Discov. 2017 November ; 7(11): 1238–1247. doi:10.1158/2159-8290.CD-17-0538.

Constitutive signaling from an engineered IL-7 receptor promotes durable tumor elimination by tumor redirected T-cells

Thomas Shum[1,5,6], **Bilal Omer**[1,2,7], **Haruko Tashiro**[1], **Robert L. Kruse**[1,5,6], **Dimitrios L. Wagner**[1], **Kathan Parikh**[1], **Zhongzhen Yi**[1], **Tim Sauer**[1], **Daofeng Liu**[1], **Robin Parihar**[1], **Paul Castillo**[1], **Hao Liu**[8], **Malcolm K. Brenner**[1], **Leonid S. Metelitsa**[1,2,3,7], **Stephen Gottschalk**[1,2,3,7], and **Cliona M. Rooney**[1,2,3,4,6]

[1]Center for Cell and Gene Therapy, Texas Children's Hospital, Houston Methodist Hospital and Baylor College of Medicine, Houston, TX, USA

[2]Department of Pediatrics, Baylor College of Medicine, Houston, Texas, USA

[3]Department of Pathology and Immunology, Baylor College of Medicine, Houston, Texas, USA

[4]Department of Molecular Virology and Microbiology, Baylor College of Medicine, Houston, Texas, USA

[5]Medical Scientist Training Program, Baylor College of Medicine, Houston, Texas, USA

[6]Interdepartmental Program in Translational Biology and Molecular Medicine, Baylor College of Medicine, Houston, TX, USA

[7]Texas Children's Cancer and Hematology Centers, Baylor College of Medicine, Houston, TX, USA

[8]Biostatistics Shared Resource, Baylor College of Medicine, Houston, TX, USA

Abstract

Successful adoptive T-cell immunotherapy of solid tumors will require improved expansion and cytotoxicity of tumor-directed T cells within tumors. Providing recombinant or transgenic cytokines may produce the desired benefits but are associated with significant toxicities, constraining clinical use. To circumvent this limitation, we constructed a constitutively signaling cytokine receptor, C7R, which potently triggers the IL-7 signaling axis but is unresponsive to extracellular cytokine. This strategy augments modified T-cell function following antigen exposure, but avoids stimulating bystander lymphocytes. Co-expressing the C7R with a tumor-directed chimeric antigen receptor (CAR) increased T-cell proliferation, survival, and anti-tumor activity during repeated exposure to tumor cells, without T cell dysfunction or autonomous T cell growth. Furthermore, C7R co-expressing CAR-T cells were active against metastatic neuroblastoma and orthotopic glioblastoma xenograft models even at cell doses that had been

Corresponding Author: Cliona Rooney, PhD., Center for Cell and Gene Therapy, Baylor College of Medicine, 1102 Bates St, Suite 1770, Houston, TX 77030, Tel: +1- 832-824-4693, Fax: +1-832-825-4732, cmrooney@txch.org.

Disclosures of Potential Conflicts of Interest: Baylor College of Medicine (TS, CMR, SG, and BO) has filed a patent application on constitutively active cytokine receptors for cell therapy.

ineffective without C7R support. C7R may thus be able to enhance antigen-specific T-cell therapies against cancer.

Keywords

T-cell immunotherapy; cancer; chimeric antigen receptors; cytokine receptors; IL-7

Introduction

Adoptive immunotherapy using T-cells modified with chimeric antigen receptors (CARs) has achieved remarkable clinical efficacy against refractory leukemia (1) and lymphoma but challenges remain in translating these successes to solid tumors. Substantial expansion and persistence of adoptively transferred T-cells are necessary for durable anti-tumor efficacy (2). Of the 3 signals required for optimal T-cell activation and expansion (3), CAR activation can recapitulate Signal 1 (T-cell receptor (TCR) activation) and Signal 2 (co-stimulation) but cannot sustain a positive Signal 3 derived from immunostimulatory cytokines that are scarce in tumor microenvironments. In xenograft tumor models, Signal 3 has been supplemented with injections of cytokines such as IL-2 to augment anti-tumor activity, without notable adverse effects (4). However, systemic administration of cytokines to cancer patients has caused significant toxicity (5–7). Alternative approaches such as genetic modification of T-cells to secrete or trans-present cytokines (8) carry a risk of severe adverse events including neurotoxicity and cytokine release syndrome from systemic accumulation of secreted cytokine (9), while T cells that overexpress cytokine receptors do not eliminate the need for exogenous cytokine (10). Therefore, a strategy to safely deliver cytokine signals to CAR T-cells remains elusive.

Here we present a strategy to selectively provide Signal 3 to T-cells with a constitutively active IL-7 cytokine receptor (C7R). This novel chimeric receptor provides signal 3 without the requirement for exogenous agents or the non-specific bystander T-cell activation caused by forced expression of transgenic cytokines. The growth and survival of C7R-expressing CAR T-cells remains antigen dependent, but in the presence of tumor, these cells have superior anti-tumor activity in multiple model systems.

Results

C7R constitutively activates STAT5 and is engineered to be unresponsive to extracellular ligand

We chose to focus our attention on IL-7, since the cytokine bolsters the persistence of tumor-specific T-cells (11), and T-cells genetically modified to either secrete IL-7 or overexpress the IL-7 receptor (in conjunction with administered IL-7) display enhanced anti-tumor efficacy in preclinical models (10,12). Recently, constitutively active IL-7 receptors have been reported to transmit IL-7 signaling without the need for ligand or the common receptor gamma chain (γ_c), as a result of IL-7Rα homodimerization due to cysteine and/or proline insertions in the transmembrane domain (13,14). Once the homodimer is formed, cross-phosphorylation of JAK1/JAK1 activates STAT5 (15), a core signaling node downstream of

IL-7. To discover whether this class of receptors could produce a consistent Signal 3 to complete the three-signal requirement for optimal CAR T-cell activity, we selected a constitutively active IL-7 receptor variant (IL7R*) that has significant STAT5 activation (16). To avoid additional activation of the receptor by external ligand and provide a means of detecting transduced cells, we replaced the native extracellular domain of the receptor with ectodomains derived from CD34. To learn whether ectodomain size factored into the efficiency of protein expression and function we used ectodomains from Q8 (65 amino acids) (17) and CD34 (259 amino acids). The Q8 ectodomain consists of a CD34 epitope mounted on top of a CD8 spacer, allowing detection by the anti-CD34 antibody clone QBEND10. Retroviral-mediated expression of the CD34-IL7R* and Q8-IL7R* constructs in healthy donor T-cells revealed poor expression of the Q8-IL7R* fusion protein and suboptimal STAT5 activation (Supplementary Figure 1). In contrast, CD34-IL7R* was robustly expressed in T-cells and was functionally active. Therefore we used CD34-IL7R*, henceforth referred to as C7R, for all subsequent experiments (Figure 1A).

To determine the relative effects of C7R in CD4 and CD8 T-cells, we separated the two subpopulations using antibody coated magnetic beads, activated and transduced them, and cultured the T-cell subsets separately from each other. We found that C7R was readily expressed by both CD4 and CD8 T-cells (Figure 1B,C and Supplementary Figure 2), and produced greater constitutive activation of STAT5 in T-cells than a control construct consisting of a truncated CD34 (Δ34) molecule (18) (Figure 1D–G). Importantly, C7R did not promote antigen-independent expansion of CD4 and CD8 T-cells *in vitro* (Figure 1H,I). While C7R transduced cells persisted significantly longer in antigen and cytokine depleted conditions than control cells *in vitro*, the C7R population began to contract by 14–21 days, with all cells dying by day 70 after initiation of the persistence assay. This confirmed that C7R does not sustain autonomous T-cell expansion, an important property for safety.

C7R promotes survival in GD2-CAR T-cells during serial *in vitro* tumor cell challenges

To evaluate whether C7R could increase anti-tumor efficacy of CAR T-cells, we treated GD2+ neuroblastoma cells with T-cells expressing a GD2-CAR comprised of a 14g2a scFv linked to a CD8α stalk and transmembrane domain, and a 41BB.ζ signaling endodomain (Supplementary Figure 3A). 14g2a-based GD2-CAR T-cells have shown a safe profile in clinical trials treating neuroblastoma patients (19,20), and while complete remissions haven been achieved in select patients, higher efficacy remains desirable. In comparing T-cells expressing either the GD2-CAR alone or a bicistronic construct containing the GD2-CAR and C7R (GD2-CAR.C7R), we found that C7R did not induce significant differences in the memory subset composition or the CD4/CD8 percentages of GD2-CAR T-cells (Supplementary Figure 3B–D). Autonomous expansion of GD2-CAR.C7R T-cells was also absent (Supplementary Figure 4). While C7R increased secretion of IFN-γ and TNF-α in GD2-CAR T-cells after stimulation with LAN-1 tumors (Figure 2A), this was not associated with any increase in the potency of T-cell killing during a 4-hour cytotoxicity assay (Figure 2B). However, GD2-CAR.C7R T-cells significantly outperformed GD2-CAR T-cells when we measured their ability to maintain cytotoxicity and expansion after repeated encounters with tumors during *in vitro* sequential co-culture killing assays (Figure 2C). We found that GD2-CAR T-cells failed by the third challenge, losing both their ability to expand and

eliminate tumor cells (Figure 2D,E). In contrast, GD2-CAR T-cells expressing C7R responded to all 3 sequential tumor challenges. To determine the relative contributions of increased proliferation versus reduced apoptosis to the improved cell expansion of GD2-CAR.C7R T-cells, we used Cell Trace Violet labeling after the first co-culture. Upon subsequent re-stimulation with tumor cells, we found that GD2-CAR.C7R T-cells showed greater cell division than T-cells expressing only the GD2-CAR (Figure 2F,G). To assess whether C7R also reduced T cell apoptosis, we used Annexin V and 7-AAD staining following the second tumor restimulation. Flow cytometric analyses showed larger populations of Annexin V(+)/7-AAD(+) GD2-CAR T cells compared to GD2-CAR.C7R T-cells (Figure 2H), demonstrating increased viability generated by C7R despite sequential tumor challenges. To further understand the molecular basis for these results, we used Nanostring technology to perform gene expression analysis of GD2-CAR and GD2-CAR.C7R T-cells after the second tumor restimulation (Figure 2I and Supplemental Table 1). *BCL2*, which mediates the anti-apoptotic effects of IL-7 (21,22), was one of the top genes upregulated by C7R in GD2-CAR T-cells. We also found upregulation of cytolytic *GZMA* and downregulation of pro-apoptotic *FAS* and *CASP8*, which are involved in cellular apoptosis and activation induced cell death (AICD) (23). Therefore, C7R augments both proliferation and survival of GD2-CAR T-cells to enhance their performance during sequential encounters with tumor cells.

C7R co-expression in CAR T-cells enhances their anti-tumor activity against xenograft tumor models

We next tested the ability of C7R-enhanced GD2-CAR T-cells to eradicate metastatic neuroblastoma in a xenograft model. We engrafted neuroblastoma cells in nonobese diabetic (NOD) severe/combined immunodeficient (SCID) IL-2r$\gamma^{-/-}$ (NSG) mice by intravenous injection of the multidrug-resistant, MYC-N non-amplified neuroblastoma cell line CHLA-255 modified to express firefly luciferase (CHLA-255 FFluc) (24). Treatment with a low dose of GD2-CAR T-cells one week after tumor engraftment increased median survival by one week, compared to control mice treated with T-cells expressing an irrelevant CAR. Mice receiving T cells expressing C7R and a non-functional GD2-CAR with a truncated endodomain (GD2-CARΔ.C7R) had identical survival to the control mice. (Figure 3A,B). In contrast, disease was eliminated in mice infused with GD2-CAR.C7R T-cells. In a parallel experiment in which T-cells rather than CHLA-255 cells were GFP-FFluc transduced, we saw no expansion of GD2-CAR T-cells with the limited dose that we infused but observed robust expansion of GD2-CAR.C7R T-cells with accumulation of T-cell signal in the liver, a site of extensive neuroblastoma metastasis (Figure 3C,D). These results demonstrated that GD2-CAR T-cells could not persist against tumors *in vivo* whereas GD2-CAR T-cells expressing C7R could proliferate and survive to mediate metastatic tumor clearance.

To investigate whether C7R could augment the performance of other CAR T-cells, we co-expressed the molecule with an EphA2-CAR intended to treat glioblastoma (25). U373 glioblastoma cells genetically modified with GFP-FFluc were injected intracranially into SCID mice. Seven days later, we administered intratumorally 10^4 EphA2-CAR T-cells, a cell dose at which gliomas could not be eradicated based on our previous experience (unpublished data). Glioblastoma bioluminescence increased rapidly in mice treated with

control T-cells co-expressing C7R and a non-functional EphA2-CAR (EphaA2-CARΔ.C7R) and no significant improvement in anti-tumor control was seen in mice receiving EphA2-CAR T-cells (Figure 3E,F). In contrast, tumors were completely eliminated in mice infused with the low "stress" dose of EphA2-CAR T-cells when they co-expressed C7R (EphA2-CAR.C7R) and these mice remained disease-free at the conclusion of the experiment. When we repeated the experiment using EphA2-CAR T-cells transduced also with GFP-FFluc, bioluminescent signal from T-cells expressing the CAR alone had largely dissipated 4–6 days after infusion. In comparison, while EphA2-CAR.C7R T-cells lacked the significantly greater expansion observed in the (extracranial) neuroblastoma models, there was a trend towards greater T-cell persistence as determined by area under the curve (AUC) comparison between EphA2-CAR and EphA2-CAR.C7R T-cells (Supplementary Figure 5).

GD2-CAR.C7R T-cells can be efficiently deleted using iC9 after tumor clearance

Although C7R expressing CAR T-cells do not show sustained autonomous/antigen independent growth and survival *in vitro* (Figure 1H,I), the transgene is modified from a class of constitutively active IL7R variants expressed in 10% of pre-T-cell acute leukemias (26), potentially increasing the risk of unwanted expansion. However, expression of this mutant receptor per se is not oncogenic, and transformation only occurs in association with multiple other driver mutations (27). Moreover, these mutational events are oncogenic only in pre-T-cell leukemia and have not been reported in the mature, post thymic T-cells that are the target cell population for most adoptively transferred T-cell products, including our current approach. As an additional safety measure, however, we generated T-cells co-expressing a clinically validated inducible caspase9 (iC9) suicide gene (28) that can electively eliminate T-cells. After double transduction with iC9 and GD2-CAR.C7R, T-cells remained sensitive to iC9 signaling and underwent apoptosis *in vitro* within 24 hours of exposure to the chemical inducer of dimerization AP20187 (CID) (Figure 4A). We next asked if iC9 could efficiently remove GD2-CAR.C7R T-cells *in vivo* after tumor regression. In order to evaluate T-cell activity and tumor growth simultaneously, we used a subcutaneous LAN-1 neuroblastoma model. Tumor cells were injected in the left dorsal flanks of NSG mice and 8 days later we intravenously injected 1×10^6 GD2-CAR.C7R T-cells alone or doubly transduced with iC9. Control mice received GD2-CARΔ.C7R T-cells. All T-cells were co-transduced with GFP-FFluc for *in vivo* visualization. After 3 weeks, LAN-1 tumors outgrew in control mice, which were euthanized. We found that T-cells co-expressing the GD2-CAR.C7R T-cells and iC9 vectors demonstrated similar anti-tumor efficacy and *in vivo* expansion as GD2-CAR.C7R T-cells alone (Figure 4B,C). To model T-cell deletion required to control toxicity after immunotherapy, we administered 3 doses of CID to mice beginning at 28 days after T-cell infusion within the same experimental approach. We observed a loss of T-cell bioluminescence signal (mean 93%) immediately after CID administration (Figure 4D) and the signal remained at baseline two weeks later without tumor recurrence, at which time the experiment was terminated. These results confirmed that CAR T-cells co-expressing C7R could be used together with iC9 if needed, without detriment to efficacy and permitting elective T-cell deletion.

Discussion

Our results demonstrate Signal 3 in T-cell activation is essential for sustaining the activity of CAR T-cells against solid tumors, and that constitutively active IL-7 receptors can be used to provide Signal 3 for the enhancement of adoptive immunotherapy. Under the stress of repeated antigen exposure that T-cells will likely encounter within solid malignancies, we found that only GD2-CAR T-cells co-expressing C7R were able to undergo multiple rounds of expansion and retain anti-tumor activity. The superiority of C7R-enhanced CAR T-cells was shown for two different CAR and tumor models *in vivo* in which functional CAR T-cells administered at ineffective doses could, if combined with C7R, sustain the ability to eradicate established tumors. In our metastatic neuroblastoma model, although we cannot detect tumor by bioluminescence at 1 week after inoculation, we and others have extensively confirmed that CHLA-255 xenograft tumors in immunodeficient mice are very aggressive with 100% tumor engraftment (24,29–32). Therefore the continued lack of CHLA-255 bioluminescence denotes tumor clearance rather than failure of engraftment.

Our gene expression analysis revealed that C7R-promoted survival of GD2-CAR T-cells during repeated tumor cell challenges is correlated with an increase of *BCL2* transcription and reduced expression of *FAS* and *CASP8*. This would suggest that C7R exerts a broad anti-apoptotic influence within CAR T-cells to decrease their susceptibility to AICD and is consistent with a previous study that highlighted the role of IL-7 in reducing the contraction of antigen-expanded T-cells (33).

While other studies have shown that addition of Signal 3 support will enhance CAR T-cell efficacy (12,34), the delivery of IL-7 signaling to T-cells by C7R confers two distinct advantages. As a constitutively active cytokine receptor that does not respond to external IL-7, C7R is uniquely designed to provide Signal 3 only to modified T-cells without affecting bystander immune cells. This avoids a potential mechanism for treatment-related toxicity associated with cytokine-secretion strategies for bolstering Signal 3; for example a recent clinical trial using CAR T-cells that inducibly secreted IL-12 was halted after a correlation was demonstrated between serum IL-12 escalation and manifestation of adverse effects (9). Secondly, because IL-7 signaling primarily promotes survival of T-cells (35,36) within lymphoreplete environments, synergistic activation from the CAR is required to drive proliferation and overall expansion. Consequently C7R would be expected to focus CAR T-cell expansion at tumor sites in an antigen-dependent manner and minimal proliferation should occur in tissues where the CAR is not activated. Other potential benefits from C7R include resistance to immunosuppressive agents such as TGF-β within the tumor microenvironment (37), as we have identified downregulation of TGF-βRII in GD2-CAR.C7R T-cells relative to GD2-CAR T-cells alone (Supplemental Table 1).

The low toxicity seen in a glioblastoma patient successfully treated with intraventricular IL-13Rα2 CAR T-cell infusions (38), together with our observation that C7R functionally enhanced EphA2-CAR T-cells without substantially increasing expansion in our orthotopic glioblastoma model, suggests a low risk for adverse events if the CAR T-cell and C7R combination strategy was used for glioblastoma treatment. We found no evidence that C7R could induce antigen-independent proliferation, although the NOD/SCID and NSG models

have obvious limitations for assessing the long-term fate of human T cells *in vivo* (39). The occurrence of xenogenic graft-versus-host disease (xenoGVHD) is dependent on the dose of human cells and on the donor used. Since even incipient xenoGVHD may distort the apparent potency of a human cell therapy in mice, in this study we selected donors who produce a low incidence of xenoGvHD even at high T cell doses (10^7/mouse) and administer just $\leq 10^6$ T cells. Thus we see no xenoGVHD even if T cells expand post injection; a similar threshold effect is seen after allogeneic hematopoietic stem cell transplantation in humans in which low dose donor lymphocyte infusions cause less GVHD than high doses (40,41). As added protection against potential concerns, however, we found that inclusion of a dimerizable iC9–mediated safety switch would allow deletion of CAR T-cells expressing C7R.

Given the effective application of C7R to GD2-CAR T-cells and EphA2-CAR T-cells against metastatic neuroblastoma and orthotopic glioblastoma, we believe our C7R molecule has the potential to enhance many other CAR T-cell candidates in testing today. It will be of interest to discover whether this same approach can increase the anti-tumor activity of other adoptive cell therapies for cancer including those based on the specificities of native (42) or transgenic TCRs (43) as well as those exploiting the properties of NK and NKT-cells (44), since all may respond to IL-7 supplementation.

Materials and Methods

Generation of retroviral vectors

pSFG.ΔCD34-IL7R* (pSFG.C7R)—A cDNA encoding a mutant IL-7Rα with a TTGTCCCAC insertion between base pairs 731 and 732 (IL7R*) (ref 15) was synthesized (Genscript, Piscataway, NJ). pSFG.C7R were generated by IN-Fusion (Takara, Mountainview, CA) cloning using a XhoI and MluI-digested SFG vector backbone, the IL7R* cDNA, and the entire extracellular domain of CD34 (ΔCD34), which was available in our laboratory.

pSFG.GD2-CAR, pSFG.GD2-CAR-2A-C7R (GD2-CAR.C7R), and pSFG.GD2Δ-CAR-2A-C7R (GD2-CARΔ.C7R)—A cDNA encoding a n-terminal leader peptide, the GD2-specific 14g2a single chain variable fragment (scFv), a CD8 stalk and transmembrane domain, and a 41BB.ζ endodomain was synthesized (Biobasic, Marham, ON, Canada) and cloned by IN-Fusion (Takara) cloning into a SFG retroviral vector upstream of an internal ribosomal entry site (IRES) and truncated NGFR. For *pSFG.GD2-CAR-2A-C7R*, the GD2-CAR was subcloned into a SFG vector upstream of a 2A sequence and C7R. For *pSFG.GD2Δ-CAR-2A-C7R*, the 2A-C7R was cloned downstream of a non-functional GD2-CAR available in the laboratory composed of the 14g2a scFv, a short IgG1 exodomain spacer, a CD28 transmembrane domain, and a truncated CD28 endodomain (RSKRSRLL).

pSFG.EphA2-CAR-2A-CD19t (EphA2-CAR), pSFG.EphA2-CAR-2A-C7R (EphA2-CAR.C7R), and pSFG.EphA2-CARΔ-2A-C7R (EphA2-CARΔ.C7R)—The generation of *pSFG.EphA2-CAR-2A-CD19t* encoding an EphA2-specific CAR consisting of the EphA2-specific 4H5 scFv (ref 25) and a 41BB.ζ endodomain, a 2A sequence, and CD19t is described elsewhere (unpublished data). *pSFG.EphA2-CAR-2A-C7R* was

generated by IN-Fusion (Takara) cloning replacing 2A-CD19t with 2A-C7R. For *pSFG.EphA2-CARΔ-2A-C7R,* 2A-C7R was cloned downstream of a non-functional EphA2-CAR described elsewhere (unpublished data).

pSFG.iC9-2A-CD19t—The vector was generated as previously described elsewhere (28).

All restriction enzymes were purchased from New England Biolabs (Ipswich, MA) and the sequence of all cloned constructs was verified by Seqwright (Houston, TX).

T-cell generation

Peripheral blood mononuclear cells (PBMCs) from healthy donors were obtained under a Baylor College of Medicine IRB-approved protocol with informed consent obtained in accordance to the Declaration of Helsinki. When CD4 and CD8 T-cells were individually evaluated, PBMCs were labeled with CD4 or CD8 magnetic selection beads (Miltenyi, Auburn, CA) and positively selected following the manufacturer's instructions. For T-cell activation on day 0, bulk or selected T-cells were suspended in complete medium consisting of 90% RPMI 1640 (Hyclone, Logan, UT), 10% Fetal Bovine Serum (Hyclone), and 1% Glutamax (Gibco, Grand Island, NY), and cultured in wells coated with OKT3 (CRL-8001, American Type Culture Collection [ATCC], Manassas, VA) and CD28 antibodies (BD Biosciences, San Jose, CA) for activation. IL-15 and IL-7 (Peprotech, Rocky Hill, NJ) were added one day after activation, and cells were retrovirally transduced on day 2 (45). T-cells were used for experiments beginning at 9–12 days after OKT3 and CD28 activation. High retroviral transduction rates were achieved using retroviral supernatants collected 48 hours after 293T cell transfection, spindown of 1ml of retrovirus/well in a 24 well retronectin coated plate followed by addition of 0.1 million T-cells. Viral supernatants generated by transient transfection were titered on human activated T cells by serial dilutions (Supplemental Figure 6). Average infectious units (iu)/ml ranged from 0.6 to 2×10e6/ml with a resulting multiplicity of infection (MOI) of 6 to 21 when 1 ml of viral supernatants was used to transduce 1×10e5 T cells.

Flow cytometry

Fluorochrome-conjugated antibodies were purchased from Biolegend (San Diego, CA; CCR7, CD45RO, NGFR); Abnova, (Taoyuan City, Taiwan; CD34); Thermo Fisher (Life Technologies, Frederick, MD; CD8); eBioscience (San Diego, CA; CD4); Beckman Coulter (Indianapolis, IN; CD3); BD Biosciences (CD8, CD4, CD3, CD34, Stat5 (pY694), Annexin V, 7-AAD). For surface staining, cells were incubated with antibodies for 15 minutes at 4 degrees C. Cells were acquired on a Beckman Coulter Galios (10,000 events) and analysis was performed using Flowjo 10.0.7r2 (Tree Star, Ashland, OR). Proliferation analysis was performed using Flowjo 9.3.2 (Tree Star).

Cytotoxicity assay

A 4-hour luciferase-based cytotoxicity assay was performed using the LAN-1 neuroblastoma cell line expressing GFP-Firefly luciferase (GFP-FFluc) based on a previously described protocol with minor modifications (46). Briefly, 2×10^4 LAN-1 neuroblastoma cells were plated per well in a 96 well black plate (Corning, Corning, NY). 24 hours later, CAR T-cells

were added in varying effector to target (E:T) ratios. The viable number of LAN-1 cells per well was determined using a standard curve generated by serial dilution of LAN-1 cells. The formula used to calculate the percent cytotoxicity is as follows: (Cell number in untreated well – Cell number in assay well)/(Cell number in untreated well).

Serial tumor challenge assay

0.5×10^6 LAN-1 cells and 1×10^6 T-cells transduced with GD2-CAR or GD2-CAR.C7R were co-cultured in a 24 well plate using fresh culture media without IL-15 and IL-7. Seven days later, cells were harvested either for FACs analysis or for T-cell quantification by trypan-blue exclusion. CAR T-cells were then replated at a 2:1 E:T ratio with fresh LAN-1 cells in fresh cell culture media to start the second and third tumor co-cultures. At the conclusion of the third co-culture, T-cells were counted and the co-culture was analyzed by FACS.

Quantitative flow analysis

To count antibody-stained cells, following a PBS wash, 25 μL of counting beads (Life Technologies) and 2 μL of 7-AAD were added (for dead cell exclusion), and cells were immediately analyzed. Acquisition of events was based on collection of 3000 counting beads.

Analysis of cytokine production

T-cells expressing GD2-CAR or GD2-CAR.C7R were cultured with LAN-1 cells using a 1:4 E:T ratio in a 24-well plate in complete culture medium without cytokines. 24 hours later, supernatants were harvested. IFN-γ and TNF-α release was quantitated using ELISA kits (R&D Systems, Minneapolis, MN).

Phosphorylated-STAT5 assay

Transduced T-cells were harvested and re-suspended at 0.5×10^6 cells/mL of complete medium without cytokines, then plated at 0.5×10^6 cells per well in a 48-well tissue cultured plate. 24–72 hours later, cells were harvested into a FACs tube and washed in cold flow buffer (PBS containing 5% FBS). 100 μL of Fix & Perm Reagent A (Life Technologies) was added to the cells, gently vortexed, and incubated for 3 minutes at room temperature before 3 mL of ice-cold methanol was slowly added to the tube with constant vortexing. The tubes were then incubated for 10 minutes at 4 degrees C. Afterwards, the tubes were centrifuged and the methanol was discarded, followed by another wash step with cold flow buffer. 100 μL of Fix & Perm Reagent B (Life Technologies) and 5 μL of anti-STAT5 antibody were then added to the cells. The cells were gently vortexed then incubated in the dark for 30 minutes at room temperature. Afterwards, the cells were washed one more time with cold flow buffer and then immediately analyzed.

Cell Trace Violet Proliferation assay

After a single co-culture with LAN-1 tumor cells, GD2-CAR T-cells and GD2-CAR.C7R T-cells were labeled with Cell Trace Violet using the kit purchased from Thermo Fisher in accordance with the manufacturer's instructions. T-cells were then re-challenged with tumor cells for 1 week before analysis. 7-AAD was added to exclude dead cells.

Apoptosis analysis

Cells were incubated with Annexin V antibody and 7-AAD, and analyzed by flow cytometry. For experiments with iC9, the chemical inducer of dimerization (CID), AP20187, was purchased from Takara Clontech.

Cell lines

LAN-1 and U373 were purchased from ATCC and used to generate LAN-1 GFP-FFluc and U373 GFP-FFluc. CHLA-255 and CHLA-255 FFluc were established and maintained as previously described (31). Routine mycoplasma surveillance was performed using an enzyme-based assay (Lonza, Rockland, ME) and cells were authenticated within a year of the experiments described using STR profiling.

Gene expression analysis

Total RNA was collected using the Qiazol reagent and the miRNeasy Micro Kit (Qiagen, Germantown, MD). Gene expression analysis used the Immunology Panel version 2 (NanoString, Seattle, WA) at the Baylor College of Medicine Genomic and RNA Profiling Core using the nCounter Analysis System. Data was analyzed using nSolver 3.0 software (NanoString). The GEO accession number for the dataset is GSE102567.

In-vivo experiments

All animal experiments followed a protocol approved by the Baylor College of Medicine Institutional Animal Care and Use Committee.

Subcutaneous neuroblastoma mouse model—10–14 week old female NSG mice were implanted subcutaneously in the dorsal left flank with 2 million LAN-1 neuroblastoma cells in 100 μL of basement membrane Matrigel (Corning). 8 days later, mice were divided into groups based on tumor sizes such that the group tumor means and variances were similar. They were then injected intravenously with 1 million GD2-CAR T-cells (10–12 days after PBMC isolation). Tumor sizes were measured twice a week with calipers and the mice were imaged for bioluminescence signal from T-cells at the same time points using the IVIS® system (IVIS, Xenogen Corporation, Alameda, CA) 10–15 minutes after 150 mg/kg D-luciferin (Xenogen) per mouse was injected intraperitoneally. The mice were euthanized when the tumor diameter was equal to or greater than 15 mm, or when the tumor exceeded 10% of the mouse body weight.

Metastatic neuroblastoma mouse model—10–14 week old female NSG mice were intravenously injected with 1 million Firefly-luciferase expressing CHLA-255 cells (CHLA-255 FFluc). 7 days later, mice were injected intravenously with 1 million GD2-CAR T-cells (10–12 days after PBMC isolation). In parallel experiments, tumor growth or T-cell expansion was indirectly assessed by weekly bioluminescent imaging as described above. In the experiments where tumor growth was tracked, mice groups were not standardized for tumor burden because CHLA-255 FFluc luminescence was not detectable at the time of T-cell injection.

Orthotopic glioblastoma mouse model—10^5 U373 glioblastoma cells were established intracranially in 8-week-old male ICR-SCID mice as previously described (25). 7 days after tumor engraftment, 10^4 T-cells were injected intracranially directly into tumors. Tumor growth or T-cell expansion was assessed by weekly bioluminescent imaging as described above. Mice in tumor growth experiments were standardized for tumor burden but not variances.

Statistical analysis

Graphs and statistics were generated using Prism 5.0 software for Windows (Graphpad Software Inc., La Jolla, CA). Measurement data are presented as mean ± standard error of the mean (SEM). The differences between means were tested using the paired two-tailed t-test. For the mouse experiments, changes in tumor radiance from baseline at each time point were calculated and compared between groups using a two-tailed paired t-test or Welch's t-test, when appropriate. 1-way ANOVA and Bartlett's test for equal variances was used when appropriate to ensure similar tumor means and variances between groups. Survival determined from the time of tumor cell injection was analyzed by the Kaplan-Meier method and differences in survival between groups were compared by the log-rank test.

Supplementary Material

Refer to Web version on PubMed Central for supplementary material.

Acknowledgments

This work was supported by P01CA094237, 1RO1CA173750, an Alex's Lemonade Stand Foundation Reach grant as well as T32DK060445 and HL092332 that supported Thomas Shum. We would like to acknowledge David Rowley and Farrah Kheradmand for helpful discussion. We would also like to acknowledge Gianpiettro Dotti and Barbara Savoldo for generously providing constructs and for helpful discussion. This work was funded in part by the Howard Hughes Medical Institutes Med into Grad Initiative. It was also supported by the Cytometry and Cell Sorting Core at Baylor College of Medicine with funding from the NIH (P30 AI036211, P30 CA125123, and S10 RR024574) and the expert assistance of Joel M. Sederstrom.

References

1. Maude SL, Frey N, Shaw PA, Aplenc R, Barrett DM, Bunin NJ, et al. Chimeric Antigen Receptor T Cells for Sustained Remissions in Leukemia. N Engl J Med. 2014:1507–17. [PubMed: 25317870]
2. Lim, WA., June, CH. Cell. Vol. 168. Elsevier Inc; 2017. The Principles of Engineering Immune Cells to Treat Cancer; p. 724-40.
3. Kershaw MH, Westwood JA, Darcy PK. Gene-engineered T cells for cancer therapy. Nat Rev Cancer Nature Publishing Group. 2013; 13:525–41.
4. Overwijk WW, Theoret MR, Finkelstein SE, Surman DR, de Jong LA, Vyth-Dreese FA, et al. Tumor regression and autoimmunity after reversal of a functionally tolerant state of self-reactive CD8+ T cells. J Exp Med. 2003; 198:569–80. [PubMed: 12925674]
5. Sportès C, Babb RR, Krumlauf MC, Hakim FT, Steinberg SM, Chow CK, et al. Phase I study of recombinant human interleukin-7 administration in subjects with refractory malignancy. Clin Cancer Res. 2010; 16:727–35. [PubMed: 20068111]
6. Conlon KC, Lugli E, Welles HC, Rosenberg SA, Fojo AT, Morris JC, et al. Redistribution, hyperproliferation, activation of natural killer cells and CD8 T cells, and cytokine production during first-in-human clinical trial of recombinant human interleukin-15 in patients with cancer. J Clin Oncol. 2015; 33:74–82. [PubMed: 25403209]

7. Brudno JN, Kochenderfer JN. Toxicities of chimeric antigen receptor T cells: recognition and management. Blood. 2016; 127:3321–31. [PubMed: 27207799]
8. Hurton LV, Singh H, Najjar AM, Switzer KC, Mi T, Maiti S, et al. Tethered IL-15 augments antitumor activity and promotes a stem-cell memory subset in tumor-specific T cells. Proc Natl Acad Sci. 2016; 113:E7788–97. [PubMed: 27849617]
9. Zhang L, Morgan RA, Beane JD, Zheng Z, Dudley ME, Kassim SH, et al. Tumor-infiltrating lymphocytes genetically engineered with an inducible gene encoding interleukin-12 for the immunotherapy of metastatic melanoma. Clin Cancer Res. 2015; 21:2278–88. [PubMed: 25695689]
10. Vera JF, Hoyos V, Savoldo B, Quintarelli C, Giordano Attianese GMP, Leen AM, et al. Genetic manipulation of tumor-specific cytotoxic T lymphocytes to restore responsiveness to IL-7. Mol Ther. 2009; 17:880–8. [PubMed: 19259067]
11. Melchionda F, Fry TJ, Milliron MJ, McKirdy MA, Tagaya Y, Mackall CL. Adjuvant IL-7 or IL-15 overcomes immunodominance and improves survival of the CD8+ memory cell pool. J Clin Invest. 2005; 115:1177–87. [PubMed: 15841203]
12. Markley JC, Sadelain M. IL-7 and IL-21 are superior to IL-2 and IL-15 in promoting human T cell-mediated rejection of systemic lymphoma in immunodeficient mice. Blood. 2010; 115:3508–19. [PubMed: 20190192]
13. Zhang J, Ding L, Holmfeldt L, Wu G, Heatley SL, Payne-Turner D, et al. The genetic basis of early T-cell precursor acute lymphoblastic leukaemia. Nature Nature Publishing Group. 2012; 481:157–63.
14. Shochat C, Tal N, Bandapalli OR, Palmi C, Ganmore I, te Kronnie G, et al. Gain-of-function mutations in interleukin-7 receptor-α (IL7R) in childhood acute lymphoblastic leukemias. J Exp Med. 2011; 208:901–8. [PubMed: 21536738]
15. Shochat C, Tal N, Gryshkova V, Birger Y, Bandapalli OR, Cazzaniga G, et al. Novel activating mutations lacking cysteine in type I cytokine receptors in acute lymphoblastic leukemia. Blood. 2014; 124:106–10. [PubMed: 24787007]
16. Zenatti PP, Ribeiro D, Li W, Zuurbier L, Silva MC, Paganin M, et al. Oncogenic IL7R gain-of-function mutations in childhood T-cell acute lymphoblastic leukemia. Nat Genet. 2011; 43:932–9. [PubMed: 21892159]
17. Philip B, Kokalaki E, Mekkaoui L, Thomas S, Straathof K, Flutter B, et al. A highly compact epitope-based marker/suicide gene for easier and safer T-cell therapy. Blood. 2014; 124:1277–87. [PubMed: 24970931]
18. Quintarelli C, Vera JF, Savoldo B, Attianese GMPG, Pule M, Foster AE, et al. Co-expression of cytokine and suicide genes to enhance the activity and safety of tumor-specific cytotoxic T lymphocytes. Blood. 2007; 110:2793–802. [PubMed: 17638856]
19. Pule MA, Savoldo B, Myers GD, Rossig C, Russell HV, Dotti G, et al. Virus-specific T cells engineered to coexpress tumor-specific receptors: persistence and antitumor activity in individuals with neuroblastoma. Nat Med. 2008; 14:1264–70. [PubMed: 18978797]
20. Louis CU, Savoldo B, Dotti G, Pule M, Yvon E, Myers GD, et al. Antitumor activity and long-term fate of chimeric antigen receptor-positive T cells in patients with neuroblastoma. Blood. 2011; 118:6050–6. [PubMed: 21984804]
21. Maraskovsky E, O'Reilly LA, Teepe M, Corcoran LM, Peschon JJ, Strasser A. Bcl-2 can rescue T lymphocyte development in interleukin-7 receptor-deficient mice but not in mutant rag-1−/− mice. Cell. 1997; 89:1011–9. [PubMed: 9215624]
22. Akashi K, Kondo M, von Freeden-Jeffry U, Murray R, Weissman IL. Bcl-2 rescues T lymphopoiesis in interleukin-7 receptor-deficient mice. Cell. 1997; 89:1033–41. [PubMed: 9215626]
23. Krammer PH, Arnold R, Lavrik IN. Life and death in peripheral T cells. Nat Rev Immunol. 2007; 7:532–42. [PubMed: 17589543]
24. Heczey A, Liu D, Tian G, Courtney AN, Wei J, Marinova E, et al. Invariant NKT cells with chimeric antigen receptor provide a novel platform for safe and effective cancer immunotherapy. Blood. 2014; 124:2824–33. [PubMed: 25049283]
25. Chow KKH, Naik S, Kakarla S, Brawley VS, Shaffer DR, Yi Z, et al. T cells redirected to EphA2 for the immunotherapy of glioblastoma. Mol Ther. 2013; 21:629–37. [PubMed: 23070117]

26. Yokoyama K, Yokoyama N, Izawa K, Kotani A, Harashima A, Hozumi K, et al. In vivo leukemogenic potential of an interleukin-7 receptor α chain mutant in hematopoietic stem and progenitor cells. Blood. 2013; 122:4259–63. [PubMed: 24174626]
27. Belver L, Ferrando A. The genetics and mechanisms of T cell acute lymphoblastic leukaemia. Nat Rev Cancer. 2016; 16:494–507. [PubMed: 27451956]
28. Di Stasi A, Tey SK, Dotti G, Fujita Y, Kennedy-Nasser A, Martinez C, et al. Inducible apoptosis as a safety switch for adoptive cell therapy. N Engl J Med. 2011; 365:1673–83. [PubMed: 22047558]
29. Song L, Ara T, Wu HW, Woo CW, Reynolds CP, Seeger RC, et al. Oncogene MYCN regulates localization of NKT cells to the site of disease in neuroblastoma. J Clin Invest. 2007; 117:2702–12. [PubMed: 17710228]
30. Song L, Asgharzadeh S, Salo J, Engell K, Wu H, Sposto R, et al. V α 24-invariant NKT cells mediate antitumor activity via killing of tumor-associated macrophages. J Clin Invest. 2009; 119:1524–36. [PubMed: 19411762]
31. Liu D, Song L, Wei J, Courtney AN, Gao X, Marinova E, et al. IL-15 protects NKT cells from inhibition by tumor-associated macrophages and enhances antimetastatic activity. J Clin Invest. 2012; 122:2221–33. [PubMed: 22565311]
32. Tian G, Courtney AN, Jena B, Heczey A, Liu D, Marinova E, et al. CD62L+ NKT cells have prolonged persistence and antitumor activity in vivo. J Clin Invest. 2016; 126:2341–55. [PubMed: 27183388]
33. Nanjappa SG, Walent JH, Morre M, Suresh M. Effects of IL-7 on memory CD8+ T cell homeostasis are influenced by the timing of therapy in mice. J Clin Invest. 2008; 118:1027–39. [PubMed: 18246202]
34. Pegram HJ, Lee JC, Hayman EG, Imperato GH, Tedder TF, Sadelain M, et al. Tumor-targeted T cells modified to secrete IL-12 eradicate systemic tumors without need for prior conditioning. Blood. 2012; 119:4133–41. [PubMed: 22354001]
35. Bradley LM, Haynes L, Swain SL. IL-7: Maintaining T-cell memory and achieving homeostasis. Trends Immunol. 2005; 26:172–6. [PubMed: 15745860]
36. Mackall CL, Fry TJ, Gress RE. Harnessing the biology of IL-7 for therapeutic application. Nat Rev Immunol Nature Publishing Group. 2011; 11:330–42.
37. Pickup M, Novitskiy S, Moses HL. The roles of TGFβ in the tumour microenvironment. Nat Rev Cancer. 2013; 13:788–99. [PubMed: 24132110]
38. Brown CE, Ph D, Alizadeh D, Ph D, Starr R, Ostberg JR, et al. Regression of Glioblastoma after Chimeric Antigen Receptor T-Cell Therapy. N Engl J Med. 2016; 375:2561–9. [PubMed: 28029927]
39. Singh N, Liu X, Hulitt J, Jiang S, June CH, Grupp SA, et al. Nature of Tumor Control by Permanently and Transiently Modified GD2 Chimeric Antigen Receptor T Cells in Xenograft Models of Neuroblastoma. Cancer Immunol Res. 2014; 2:1059–70. [PubMed: 25104548]
40. Chalandon Y, Passweg JR, Schmid C, Olavarria E, Dazzi F, Simula MP, et al. Outcome of patients developing GVHD after DLI given to treat CML relapse: a study by the chronic leukemia working party of the EBMT. Bone Marrow Transplant. 2010; 45:558–64. [PubMed: 19633691]
41. Bar M, Sandmaier BM, Inamoto Y, Bruno B, Hari P, Chauncey T, et al. Donor Lymphocyte Infusion for Relapsed Hematological Malignancies after Allogeneic Hematopoietic Cell Transplantation: Prognostic Relevance of the Initial. Biol Blood Marrow Transplant. 2013; 19:949–57. [PubMed: 23523892]
42. Dudley ME, Yang JC, Sherry R, Hughes MS, Royal R, Kammula U, et al. Adoptive cell therapy for patients with metastatic melanoma: Evaluation of intensive myeloablative chemoradiation preparative regimens. J Clin Oncol. 2008; 26:5233–9. [PubMed: 18809613]
43. Obenaus M, Leitão C, Leisegang M, Chen X, Gavvovidis I, van der Bruggen P, et al. Identification of human T-cell receptors with optimal affinity to cancer antigens using antigen-negative humanized mice. Nat Biotechnol. 2015; 33:402–7. [PubMed: 25774714]
44. Pellegrini M, Calzascia T, Elford AR, Shahinian A, Lin AE, Dissanayake D, et al. Adjuvant IL-7 antagonizes multiple cellular and molecular inhibitory networks to enhance immunotherapies. Nat Med. 2009; 15:528–36. [PubMed: 19396174]

45. Xu Y, Zhang M, Ramos CA, Durett A, Liu E, Dakhova O, et al. Closely related T-memory stem cells correlate with in vivo expansion of CAR.CD19-T cells and are preserved by IL-7 and IL-15. Blood. 2014; 123:3750–9. [PubMed: 24782509]

46. Liu, D., Song, L., Brawley, VS., Robison, N., Wei, J., Gao, X., et al. Clin Immunol. Vol. 149. Elsevier Inc; 2013. Medulloblastoma expresses CD1d and can be targeted for immunotherapy with NKT cells; p. 55-64.

Statement of Significance

The constitutively signaling C7R system developed here delivers potent IL-7 stimulation to CAR T-cells, increasing their persistence and anti-tumor activity against multiple preclinical tumor models, supporting its clinical development.

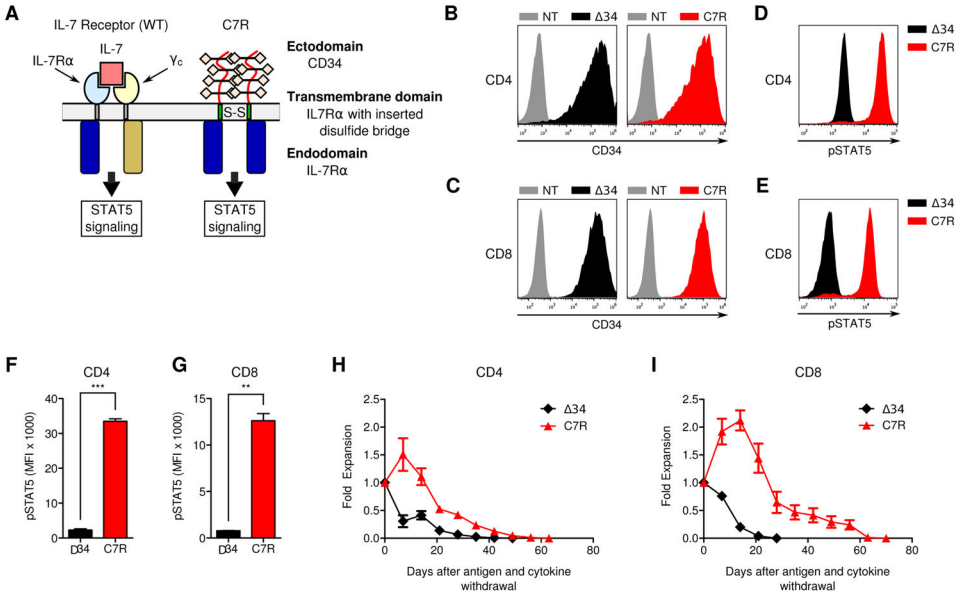

Figure 1. Constitutive signaling from C7R activates STAT5 in T-cells but does not support autonomous cell expansion

(**A**) Schematic comparisons of IL-7 bound to the natural IL-7 receptor composed of heterodimerized IL7Rα and γ_c, compared to the engineered C7R homodimerized receptor. (**B**,**C**) Transduction efficiency of Δ34 and C7R (representative of 3) in (**B**) CD4 and (**c**) CD8 T-cells relative to non-transduced (NT) cells. (**D**,**E**) Representative flow cytometric comparison of phosphorylated STAT5 (pSTAT5) in (**D**) CD4 and (**E**) CD8 T-cells that were transduced with Δ34 or C7R. Cells were cultured without IL-15 and IL-7 for 24–72 hours before analysis. (**F**,**G**) Average pSTAT5 MFI values when repeating the experiments in **D** and **E** with multiple donors. (**H**,**I**) Quantitated *in-vitro* persistence of Δ34 or C7R transduced (**H**) CD4 or (**I**) CD8 T-cells cultured in cytokine-free complete cell culture media starting 9–12 days after PBMC activation, without further antigen stimulus. Live cells were counted weekly using trypan-blue exclusion. X-axis denotes the number of days after IL-15 and IL-7 were withdrawn from culture media. Area under the curve (AUC) values were compared with the two-tailed t-test: 10.5 ± 0.6616 (CD8 Δ34), 56.37 ± 7.972 (CD8 C7R), $p<0.05$; 10.22 ± 1.694 (CD4 Δ34) and 31.36 ± 2.590 (CD4 C7R), $p<0.05$. *P<0.05, **P<0.01, ***P<0.001 (two-tailed paired t-test, **F**–**I**). Graphs **F**–**I** represent averages from different donors ± SEM (n=3).

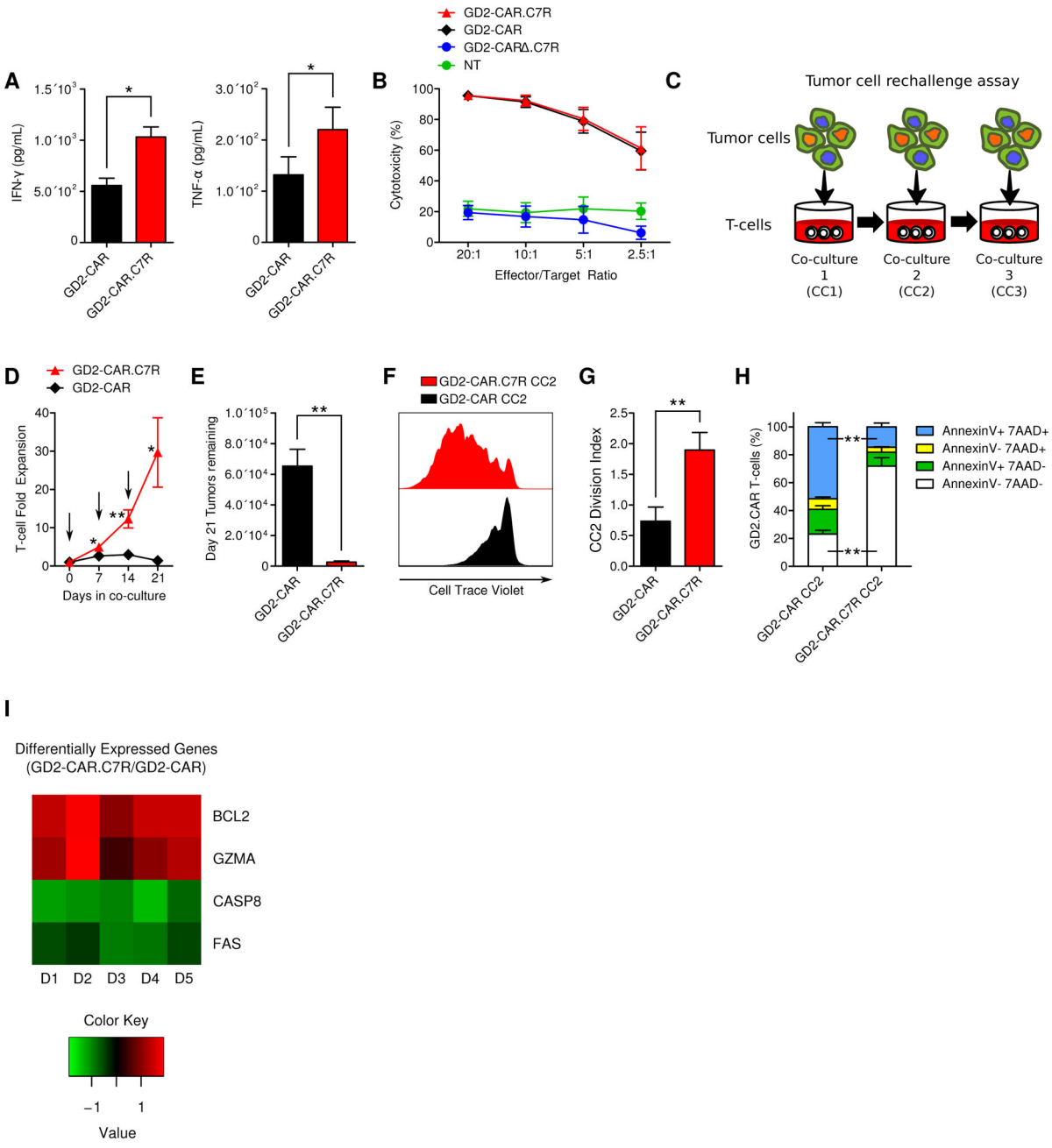

Figure 2. C7R enhances GD2-CAR T-cell activity during serial tumor challenge

(**A**) Cytokines secreted by GD2-CAR T-cells or GD2-CAR.C7R T-cells 24 hours after co-culture with LAN-1 tumor cells was determined by ELISA. (**B**) 4-hour luciferase-based cytotoxicity assay of T-cells killing LAN-1 tumor cells. (**C**) Serial co-culture schematic. The first co-culture (CC1) was initiated with 1×10^6 GD2-CAR or GD2-CAR.C7R T-cells together with 0.5×10^6 LAN-1 GFP-FFluc tumor cells for 7 days, in the absence of IL-15 or IL-7. For the second and third co-cultures (CC2 and CC3), T-cells were harvested from the previous co-culture and then replated in new culture medium with fresh tumor cells at the same 2:1 E:T ratio. (**D**) Cumulative expansion of GD2-CAR or GD2-CAR.C7R T-cells

during serial co-culture. Arrows indicate timepoints of T-cell re-stimulation with tumor cells. (**E**) LAN-1 tumor cells remaining after CC3 with GD2-CAR T-cells and GD2-CAR.C7R T-cells, respectively. (**F,G**) For proliferation analysis, GD2-CAR and GD2-CAR.C7R T-cells collected at the end of CC1 were labeled with Cell Trace Violet before being rechallenged during CC2. (**F**) Histogram overlay represents data from a representative donor. (**G**) The experiment in **F** was repeated with multiple donors and the division indices compiled from the GD2-CAR and GD2-CAR.C7R proliferation histograms. (**H**) For survival analysis, GD2-CAR and GD2-CAR.C7R T-cells were stained with Annexin V and 7-AAD after 2 serial tumor challenges with LAN-1 tumor cells. Bar graphs show the frequencies of T-cells staining positive for Annexin V, 7-AAD, both, or neither. The Annexin V(+)7-AAD(−) and Annexin V(−)7-AAD(+) mean comparisons were n.s. (**I**) After the end of CC2, tumors were labeled with GD2-specific antibody and magnetically separated from the CAR T-cells. Total RNA was isolated from T-cells and gene expression analysis was subsequently performed using the Human Immunology Panel Version 2 and nCounter Analysis System (Nanostring). The displayed heat map shows genes with log2 fold changes (GD2-CAR.C7R/GD2-CAR) that had P values less than 0.02. Data was generated from 5 donors (10 paired samples). *P<0.05, **P<0.01, (two-tailed paired t-test, **A**, **B**, **D**, **E**, **G**, **H**). Graphs **A, B, C, E, G, H** represent averages from different donors ± SEM (n=6, **A, D, E**; n=3, **G, H**).

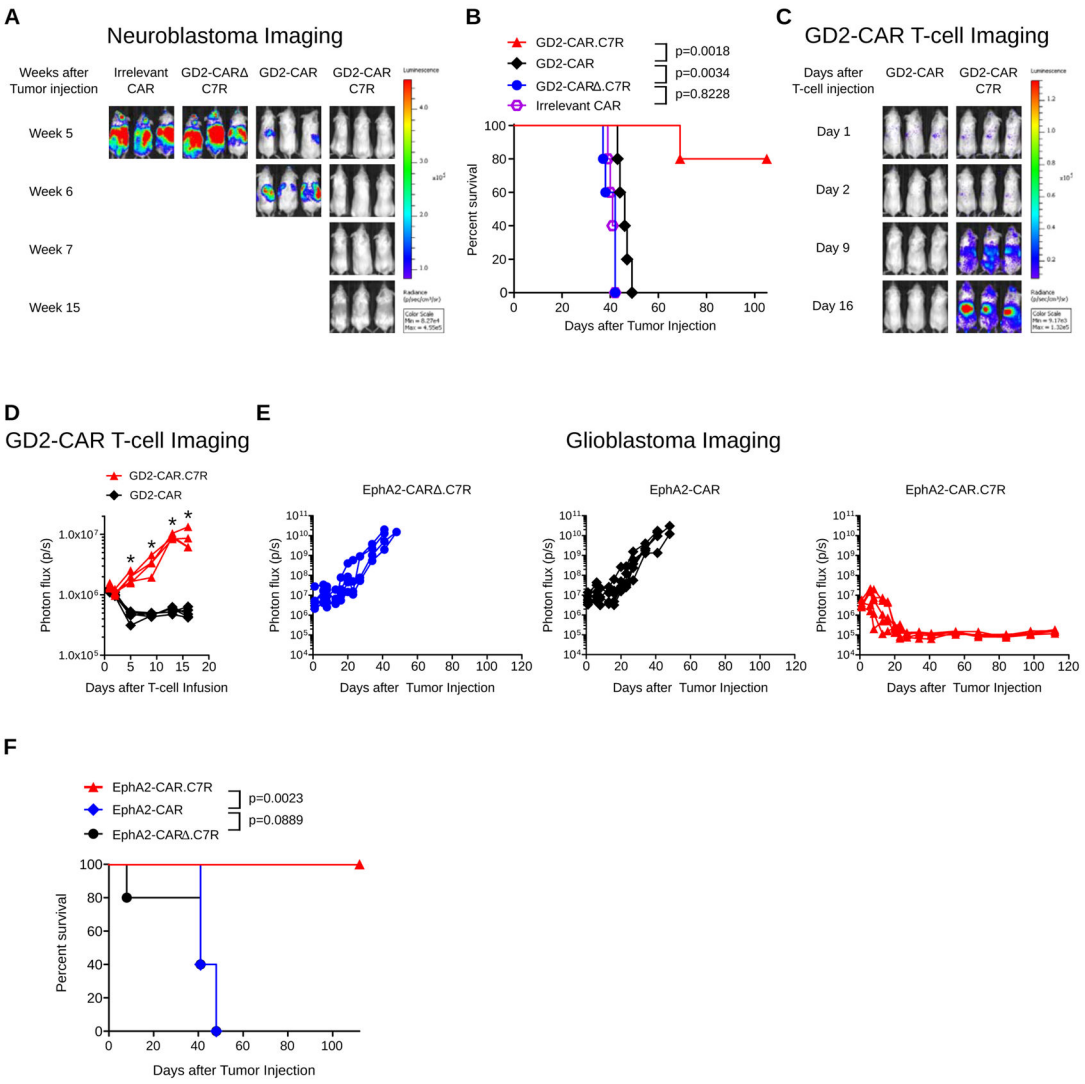

Figure 3. C7R enhances adoptive T-cell immunotherapy against metastatic and intracranial malignancies

(**A**) and (**B**) 1×10^6 CHLA-255 FFluc cells were injected i.v. into female NSG mice, followed 7 days later by 1×10^6 T-cells expressing an irrelevant CAR, GD2-CARΔ.C7R, GD2-CAR, or GD2-CAR.C7R. (**A**) Representative bioluminescent images of neuroblastoma growth over time. (**B**) Kaplan Meier survival analysis of CHLA-255 FFluc challenged mice. (**C**,**D**) To track T-cell migration and persistence, in a parallel experiment, 1×10^6 CHLA-255 cells were injected intravenously into NSG mice, followed 7 days later by 1×10^6 GFP-FFluc T-cells co-expressing GD2-CAR or GD2-CAR.C7R. (**C**) Sequential bioluminescent imaging of T-cells (**D**) Quantitated bioluminescent signal of T-cells over time (**E**) 1×10^5 U373 GFP-FFluc cells were injected intracranially into male SCID mice. 7 days later, 1×10^4 T-cells expressing EphA2-CARΔ.C7R, EphA2-CAR, or EphA2-CAR.C7R were intracranially injected into the tumor. Quantitated U373 GFP-FFluc bioluminescence from each treatment group is displayed over time. (**F**) Kaplan Meier survival analysis of U373 GFP-FFluc challenged mice after treatment with T-cells. *P<0.05 (Welch's t-test, **D**). 5 mice were used

for all groups. Graph **D** represent averages from experiment replicates ± SEM. In the experiment depicted in **D,** one mouse in the GD2-CAR.C7R group died during imaging on day 5 for reasons unrelated to tumor burden, therefore averaged bioluminescent signal in GD2-CAR.C7R for days 9–16 are computed from n=4.

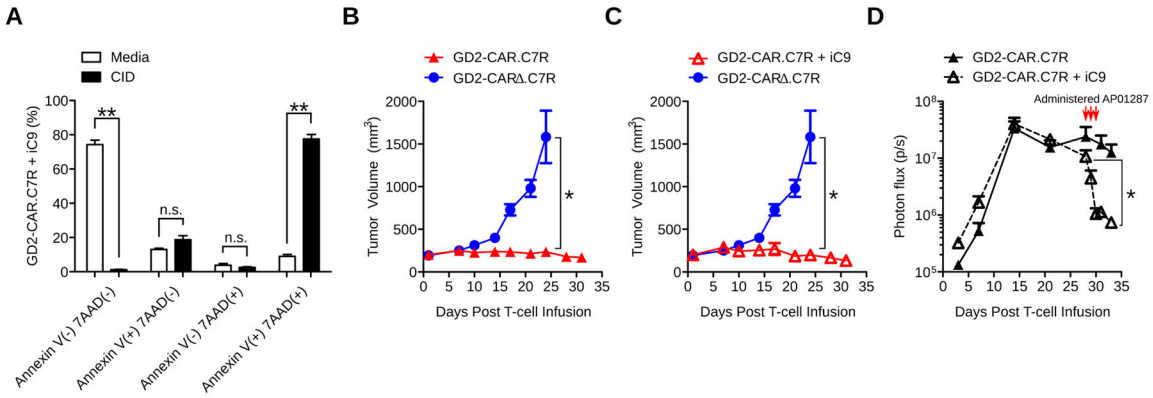

Figure 4. C7R-CAR T-cells can be deleted using the iC9 suicide switch

(**A**) T-cells doubly transduced with GD2-CAR.C7R and iC9-CD19t vectors were selected for iC9 expression using CD19-specific Miltenyi beads. Cells were then incubated with AP20187 in complete culture media for 24 hours and then stained with Annexin V and 7-AAD. Bar graphs show relative frequencies of T-cells staining positive for Annexin V, 7-AAD, both, or neither. Annexin V(+)7-AAD(−) and Annexin V(−)7-AAD(+) comparisons were n.s. (**B**,**C**) LAN-1 tumors were established subcutaneously in NSG mice for 8 days before 1×10^6 T-cells transduced with GFP-FFluc and with GD2-CARΔ.C7R, GD2-CAR.C7R, or GD2-CAR.C7R + iC9-CD19t were infused intravenously. GD2-CARΔ.C7R was used as the same control in **B** and **C**. Tumor volumes were measured over time. 2 mice in the GD2-CARΔ.C7R group were euthanized after Day 21 due to tumor burden, and on Day 24 the tumor sizes of the remaining 3 mice were compared with those in the GD2-CAR.C7R and GD2-CAR.C7R + iC9-CD19t groups. Mean tumor volume at 32 days after T-cell infusion: 236 ± 11 mm^3 for GD2-CAR.C7R, 196 ± 18 mm^3 for GD2-CAR.C7R + iC9-ΔCD19t, n.s. (p = 0.1857). (**D**) Bioluminescent signal of GD2-CAR.C7R T-cells (with and without iC9-CD19t) from the tumor site was quantitated over time. Red arrows indicate initiation of AP20187 dosing on Day 28 every 24 hours for a total of 3 doses. *P<0.05, **P<0.01 (two-tailed t-test, **A**,**D**; Welch's t-test, **B**,**C**). n=5 mice per group. The graph in **A** represents averages from different donors ± SEM (n=3).